



Deletions associated with stabilization of the Top1 cleavage complex in yeast are products of the nonhomologous end-joining pathway

Jang-Eun Cho^{a,1} and Sue Jinks-Robertson^{a,2}

^aDepartment of Molecular Genetics and Microbiology, Duke University Medical Center, Durham, NC 27710

Contributed by Sue Jinks-Robertson, September 20, 2019 (sent for review August 14, 2019; reviewed by Hannah L. Klein and Sergei M. Mirkin)

Topoisomerase I (Top1) resolves supercoils by nicking one DNA strand and facilitating religation after torsional stress has been relieved. During its reaction cycle, Top1 forms a covalent cleavage complex (Top1cc) with the nicked DNA, and this intermediate can be converted into a toxic double-strand break (DSB) during DNA replication. We previously reported that Top1cc trapping in yeast increases DSB-independent, short deletions at tandemly repeated sequences. In the current study, we report a type of DSB-dependent mutation associated with Top1cc stabilization: large deletions (median size, ~100 bp) with little or no homology at deletion junctions. Genetic analyses demonstrated that Top1cc-dependent large deletions are products of the nonhomologous end-joining (NHEJ) pathway and require Top1cc removal from DNA ends. Furthermore, these events accumulated in quiescent cells, suggesting that the causative DSBs may arise outside the context of replication. We propose a model in which the ends of different, Top1-associated DSBs are joined via NHEJ, which results in deletion of the intervening sequence. These findings have important implications for understanding the mutagenic effects of chemotherapeutic drugs that stabilize the Top1cc.

topoisomerase I | nonhomologous end joining | double-strand break | yeast

Topoisomerase I (Top1) resolves DNA torsional stress by removing supercoils that accumulate during transcription, replication, and chromatin remodeling (1). Top1 is a type IB enzyme that uses an active site tyrosine to cleave one DNA strand. This generates a transient Top1 cleavage complex (Top1cc) in which the enzyme is covalently attached to the 3' end of the nick, leaving a 5'-OH on the other side. Controlled rotation of the strand downstream of the Top1cc relaxes DNA, and subsequent attack of the 3'-phosphotyrosyl bond by the 5'-OH restores strand continuity and releases the enzyme. Top1 is the sole target of the chemotherapeutic drug camptothecin (CPT), which stabilizes the Top1cc by reversibly inhibiting the religation step (2–4). The encounter of a stabilized cleavage complex with the replication machinery converts the Top1-generated nick into a toxic double-strand break (DSB) that can trigger subsequent cell death. CPT derivatives irinotecan and topotecan thus preferentially kill rapidly dividing cells and are currently used in the clinic to treat tumors that include small-cell lung carcinoma, colorectal cancer, and ovarian cancer (5). In *Saccharomyces cerevisiae*, DSBs are predominantly repaired by homologous recombination and defects in this pathway greatly sensitize cells to the toxic effects of CPT (6, 7). The alternative nonhomologous end-joining (NHEJ) pathway is relatively inefficient and only becomes important in the absence of homologous recombination (8).

In addition to the critical role that Top1 plays during normal DNA metabolic processes, it also can be a source of spontaneous mutagenesis in yeast. This activity was initially discovered during examination of the elevated mutagenesis that accompanies very high levels of transcription (9, 10). Top1 was found to be responsible for a distinctive mutation signature composed of the deletion of a repeat unit within a small number of 2- to 5-bp

tandem repeats. Because the rate of these events is not affected by loss of homologous recombination or NHEJ, the relevant intermediate is a nick rather than a DSB. Furthermore, Top1-dependent deletions occur at distinct hot spots and most are at positions where a single ribonucleotide is embedded in DNA (11, 12). Ribonucleotide-dependent events reflect sequential cleavage of the same DNA strand by Top1, followed by enzyme-mediated religation across the resulting gap (13–15). There are events, however, that are ribonucleotide independent and are specifically elevated under conditions where the Top1cc accumulates, suggesting a second mechanism of deletion formation (11). Two conditions are known to increase Top1cc accumulation in yeast: expression of the mutant Top1-T722A protein, which has reduced religation activity compared to the wild-type (WT) enzyme (16, 17), or treatment of WT cells with CPT.

While CPT treatment increases small deletions in highly active yeast genes (18), earlier experiments in mammalian cells demonstrated that most forward mutations associated with topotecan or CPT treatment were larger-scale deletions and/or rearrangements (19, 20). In the current study, we report that either expression of Top1-T722A or treatment of WT haploid yeast cells with CPT likewise generates large deletions in a frameshift-reversion assay. The median deletion size was ~100 bp, although

Significance

The separation of DNA strands during replication and transcription creates torsional stress (supercoiling) that requires resolution by topoisomerases. Topoisomerase 1 (Top1) removes supercoils by transiently nicking one DNA strand, which allows its rotation around the intact, complementary strand. Stabilization of the covalent Top1–DNA cleavage intermediate results in potentially toxic DNA damage during replication, making this enzyme an attractive target of chemotherapeutic drugs. We find that genetic or chemical Top1 stabilization gives rise to large deletions that require the nonhomologous end-joining pathway and most likely reflect the joining of nonadjacent ends. Furthermore, the relevant Top1-mediated damage accumulates in nondividing cells, suggesting a potential mechanism for genetic change that occurs outside the context of replication.

Author contributions: J.-E.C. and S.J.-R. designed research; J.-E.C. performed research; J.-E.C. and S.J.-R. analyzed data; and J.-E.C. and S.J.-R. wrote the paper.

Reviewers: H.L.K., New York University School of Medicine; and S.M.M., Tufts University.

Competing interest: S.J.-R. and H.L.K. are coauthors on a 2019 review.

This open access article is distributed under [Creative Commons Attribution-NonCommercial-NoDerivatives License 4.0 \(CC BY-NC-ND\)](https://creativecommons.org/licenses/by-nc-nd/4.0/).

Data deposition: Python script was deposited at Github (<https://github.com/muthalpy/MHfinderatDelJct.git>).

¹Present address: Lineberger Comprehensive Cancer Center, University of North Carolina at Chapel Hill, Chapel Hill, NC 27599.

²To whom correspondence may be addressed. Email: sue.robertson@duke.edu.

This article contains supporting information online at www.pnas.org/lookup/suppl/doi:10.1073/pnas.1914081116/-DCSupplemental.

First published October 21, 2019.

deletions as large as 4 kb were detected. Genetic analyses demonstrated that large deletions require removal of the Top1cc from DNA ends and that they are products of NHEJ. Furthermore, deletions accumulated in quiescent cells, suggesting that formation of the initiating DSBs does not necessarily require DNA replication. We propose a model in which the accumulation of trapped Top1 generates multiple DSBs, with subsequent NHEJ-mediated joining of 2 different breaks resulting in deletion of the intervening sequence.

Results

The mutagenic potential of the Top1cc was examined by expressing the Top1-T722A protein, which is a well-established CPT mimic (16), in a haploid yeast strain. Prior studies using a plasmid-encoded *top1-T722A* allele fused to the *CUP1* promoter demonstrated synthetic lethality with genes involved in homologous recombination (21), consistent with conversion of the stabilized Top1cc into a toxic DSB. For our studies, the genomic *top1-T722A* allele was fused to a galactose-inducible promoter (*pGAL1*) for regulated expression. Top1cc-induced mutations were monitored using the *lys2ΔBglNR* +4 frameshift allele, the reversion of which requires a net -1 mutation (22). Compensatory mutations are generally limited to a 150-bp reversion window

defined by stop codons in the alternative reading frames. Amino acids in this region are functionally dispensable, which allows a large variety of compensatory mutations to be detected (23). Furthermore, the reversion window for the *lys2ΔBglNR* allele lacks a tandem-repeat hot spot for the Top1-dependent small deletions previously associated with transcription (9), which eliminates the occurrence of these events. Finally, because Top1 is targeted to transcribed regions through interaction with the phosphorylated C-terminal domain of elongating RNA polymerase II (24, 25), the promoter of the chromosomal *lys2ΔBglNR* reporter was replaced with the highly active *pTET* promoter (Fig. 1A). Following the selection of Lys⁺ revertants, compensatory changes were determined by sequencing the reversion window following amplification of a ~900-bp fragment.

Top1-T722A Expression Is Associated with Large Deletions. In initial experiments, cells were grown in synthetic complete medium supplemented with 2% galactose (SG) for 3 d prior to selective plating on synthetic dextrose medium deficient in lysine (SD-lys). In a *top1Δ* or *pGAL-TOP1* strain, the reversion rate of the *pTET-lys2ΔBglNR* allele was 2–3 × 10⁻⁸ (Fig. 2A and *SI Appendix, Table S1*). The reversion rate in the strain containing the *pGAL-top1-T722A* allele was elevated ~8-fold, and very strikingly, 80% (35/44) of revertants contained a large deletion (Fig. 1B and *SI Appendix,*

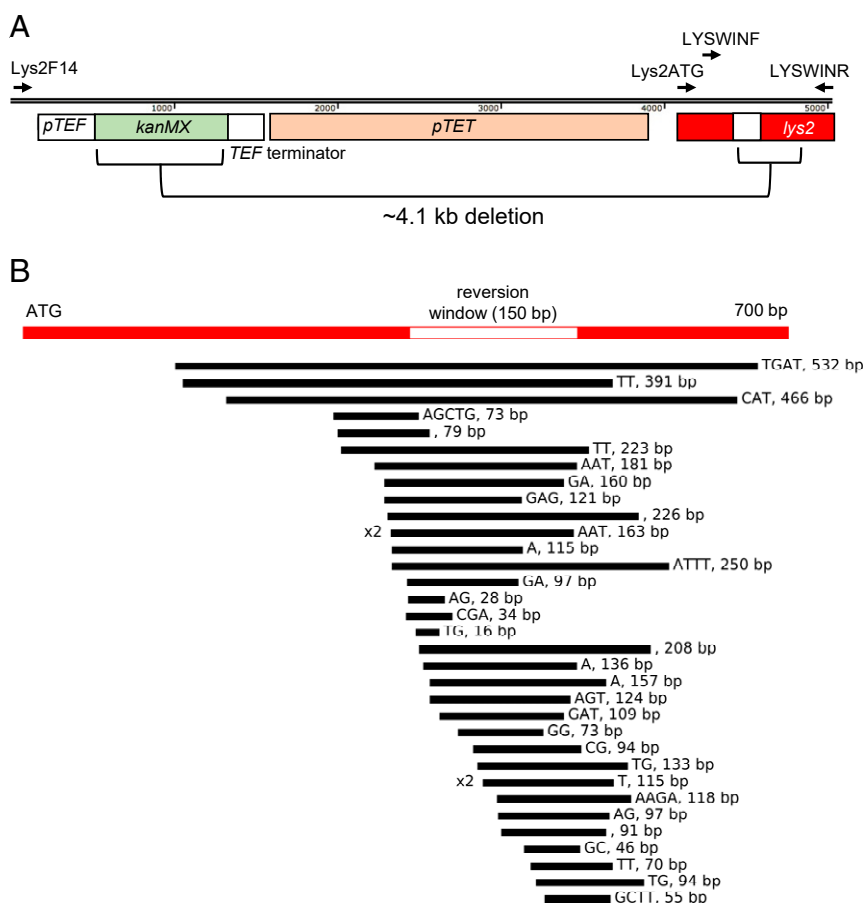


Fig. 1. Molecular features of large deletions associated with Top1-T722A expression. (A) Elements in the 4 kb upstream of the *LYS2* ORF (*pTEF-kanMX* and *pTET*) and the first 1 kb of the *lys2ΔBglNR* allele are shown. The red box corresponds to the first 700 bp of the 4.2-kb *LYS2* ORF; the white box indicates the reversion window for the *lys2ΔBglNR* allele. LYSWINF and LYSWINR were used to amplify the reversion window; when a product was not obtained, forward primers Lys2ATG and Lys2F14 were used in conjunction with LYSWINR. Brackets designate regions where the deletion endpoints for the ~4.1-kb deletions were located. Upstream endpoints were confined to *kanMX* marker, while downstream endpoints resided within or downstream of the reversion window. (B) Deletions confined to *LYS2* in WT cells grown for 3 d in SG. Black bars represent the length of individual deletion events; a number to the left of a bar indicates the number of times a given deletion was observed. The size of each deletion and the sequence of the endpoint homology is to the right of each black bar. The size and endpoint data for all deletions are visually presented in *SI Appendix, Figs. S1 and S2*, and the precise endpoints are in *SI Appendix, Table S2*.

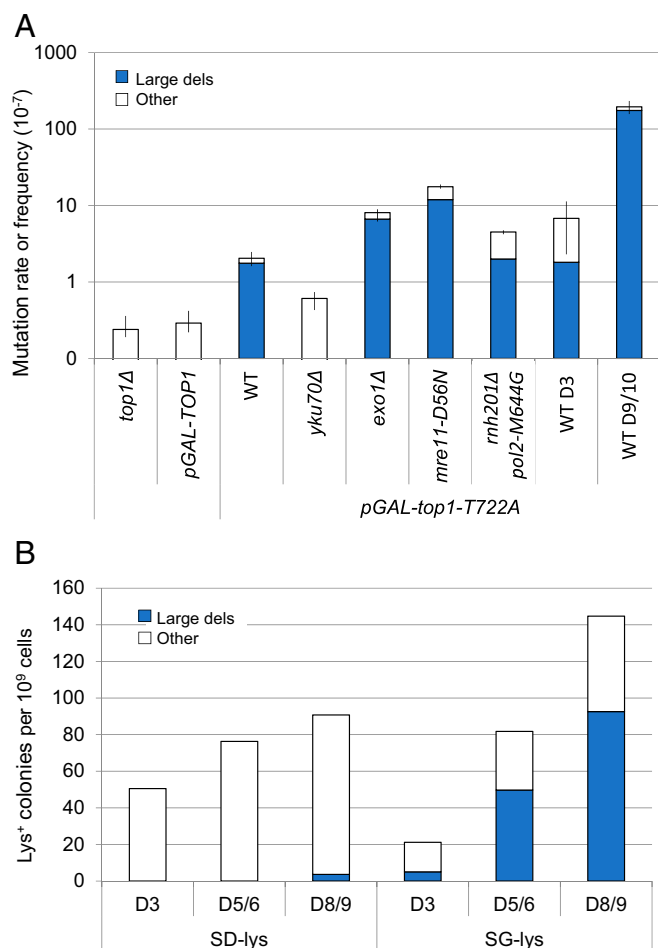


Fig. 2. Top-T722A expression is associated with large deletions. **(A)** Rate or frequency of large deletions in *pGAL-top1-T722A* cells grown in synthetic galactose (SG) medium. D3 and D9/10 data reflect the selective plating of WT cells after 3 and 9 or 10 d of nonselective growth, respectively. All other strains were grown for 3 d prior to selective plating. The total *Lys*⁺ rate or frequency with 95% confidence intervals is plotted; frequencies are given for WT D3 and WT D9/10 data and rates for the others. Filled blue areas represent the frequency of large deletions. **(B)** Time-dependent accumulation of *Lys*⁺ colonies on SD-lys and SG-lys plates. The total number of viable cells plated on SD-lys and SG-lys media was 9.7×10^8 and 16.8×10^8 , respectively. Filled blue areas are the proportion of large deletions in the corresponding spectra. Primary data for A and B are in *SI Appendix, Tables S1 and S3*, respectively.

Table S2 for deletion coordinates). We used 5 bp as the cutoff for defining a large deletion as this was the maximum size previously associated with Top1 activity in a *CAN1* forward mutation assay (9). The median large-deletion size was 115 bp, and the fusion junctions either contained no homology or only a small amount of microhomology. The largest deletion spanned the reversion window and removed 532 bp of the *LYS2* coding sequence, although most deletions were confined to or did not extend far outside this window.

In contrast to consistent amplification of genomic DNA from *Lys*⁺ colonies in other studies, ~10% (3/44) of revertants failed to yield a PCR product. Additional analyses demonstrated that these contained a ~4-kb deletion that began in or downstream of the reversion window and terminated in a *kanMX* marker that was part of the *pTET* cassette. Although the fusion endpoints were variable, all generated a functional protein that was missing the *Lys2* N terminus and presumably was expressed from the *TEF* promoter (see Fig. 1A and *SI Appendix, Fig. S1*, for a visual summary of all ~4-kb deletions, and *SI Appendix, Table S2*, for

the corresponding deletion coordinates). Because both deletion classes had similar genetic requirements, they are considered jointly in the analyses that follow.

Large Deletions Require the NHEJ Pathway. The presence of little or no homology at large-deletion junctions suggested that they were likely the result of NHEJ-mediated repair of Top1-associated DSBs. This was confirmed by deleting *YKU70*, which encodes a subunit of the Ku (Ku70–Ku80) end-protection complex that is required for NHEJ. In the *yku70Δ* background, the *Lys*⁺ rate was reduced 3.3-fold, and there was only one large deletion among the 35 revertants sequenced; this corresponds to an estimated 100-fold reduction in the large-deletion rate (Fig. 2A). Exo1 participates in the removal of the 5' ends of DSBs, and we examined whether its activity was relevant to large deletions in general and/or the 4-kb class of large deletions in particular. The rate of large deletions was elevated 3.8-fold in an *exo1Δ* background (Fig. 2A and *SI Appendix, Fig. S2* and *Tables S1 and S2*), however, demonstrating that Exo1 suppresses these events. This result, together with the strong dependence on Ku, is most consistent with a model in which *top1-T722A*-dependent large deletions reflect the joining of non-adjacent, unresected ends.

Prior studies demonstrated synthetic lethality between the *top1-T722A* allele and deletion of *MRE11* (21), which encodes a subunit of the multifunctional MRX (Mre11–Rad50–Xrs2; MRE11–RAD50–NBS1 or MRN in mammals) complex (26). In the context of MRX, the nuclease activity of Mre11 is required to remove covalently attached Spo11 following meiotic DSB formation (27) and to process damaged/blocked DNA ends during mitosis (28). Because loss of Mre11 nuclease activity confers weaker CPT sensitivity than loss of the entire protein (29), we examined whether the nuclease activity was required for survival and/or large-deletion formation in the *pGAL-top1-T722A* background. In contrast to *MRE11* deletion, the *mre11-D56N* nuclease-dead allele (27) was compatible with the *top1-T722A* allele, and its presence was associated with a 6.8-fold increase in the large-deletion rate (Fig. 2A). This increase is consistent with single-molecule studies demonstrating that human MRN releases Ku from DNA ends (30), which precludes NHEJ. Although our *mre11-D56N top1-T722A* strain was viable, synthetic lethality between *top1-T722A* and the nuclease-deficient *mre11-H125L/D126V* allele was previously reported (31). This discrepancy could reflect strain background and/or allele-specific differences.

Top1 cleavage at a single ribonucleotide embedded in duplex DNA can lead to direct DSB formation *in vitro* and *in vivo* (32). Whether Top1-T722A cleavage at ribonucleotides is a major contributor to large deletions in the current system was examined by expressing Top1-T722A in a background with an elevated genomic burden of ribonucleotides (*mh201Δ pol2-M644G* background; ref. 33). The total *Lys*⁺ reversion frequency was elevated 2.3-fold in an *mh201Δ pol2-M644G* background, but this reflected a specific increase in 4-bp deletions (19/43 versus 2/44 in WT; $P < 0.001$), consistent with the sequential-cleavage mechanism Top1-generated small deletions. Although these data exclude ribonucleotide cleavage as a major source of large deletions, we note that there was a proportional increase in the ~4-kb events (3/38 in WT versus 7/19 in the *mh201Δ pol2-M644G* mutant; $P = 0.03$ with Bonferroni correction).

Large Deletions Are Time as Well as Growth Dependent. The measurement of mutation rates by fluctuation analysis requires that independent cultures contain the same total number of cells and assumes that events occur during nonselective growth. In experiments with *pGAL-top1-T722A* strains, however, we found that continued incubation of saturated cultures was associated with the accumulation of *Lys*⁺ revertants. To further investigate this, aliquots of cultures were plated as soon as cells ceased growing (day 3 [D3]), and the remaining cells were then

incubated for an additional 6 or 7 d before selective plating (9 or 10 d postinoculation; D9/10). The median Lys^+ frequency was 29-fold higher when D9/10 cultures were plated than when D3 cultures were plated, and the proportion of deletions increased from 27% at D3 to 90% at D9/10. This corresponds to a ~100-fold increase in the frequency of large deletions between D3 and D9/10 (Fig. 2A).

The above results are consistent with the occurrence of large deletions when cells stop dividing, but also could reflect selective outgrowth of Lys^+ revertants. We thus used an alternative method to examine mutation accumulation in nondividing cells: the appearance of Lys^+ colonies as a function of time after selective plating. In this experiment, multiple independent cultures of the *pGAL-top1-T722A* strain were grown to saturation in minimal medium supplemented with dextrose in order to prevent *top1-T722A* expression. Cells were then plated in parallel on lysine-deficient galactose medium (SG-lys) to induce *top1-T722A* expression or on dextrose plates (SD-lys) to maintain repression. Lys^+ colonies were counted on D3, D5/6, and D8/9 after selective plating, and representative colonies were analyzed to determine the proportions of large deletions (Fig. 2B and *SI Appendix*, Table S3). Although there were twice as many Lys^+ colonies on SD-lys than on SG-lys plates at D3 postplating, there were proportionally more large deletions among the SG-lys colonies (5/21 on SG-lys and 0/46 on SD-lys; $P = 0.002$ by Fisher exact test). By D8/9 postplating, the number of Lys^+ colonies had increased 7-fold on SG-lys, but only 1.8-fold on SD-lys medium. There also was a further proportional increase in large deletions among Lys^+ colonies that appeared on SG-lys plates (to 103/161; $P < 0.001$), but not among those that arose on SD-lys (to 3/75; $P = 0.29$). We estimate ~20-fold more large deletions on D8/9 than on D3 when cells were plated on SG-lys medium; the number of Lys^+ colonies containing other mutation types increase only 3.2-fold between D3 and D8/9. These data are consistent with accumulation of deletions when Top1-T722A expression is limited to postmitotic cells.

Large Deletions Accumulate in Quiescent Cells. It is difficult to rule out residual cell turnover as the explanation for continued accumulation of large deletions in saturated cultures or on selective medium. To more rigorously investigate whether growth is required, we used phosphate starvation (34) to obtain cells in a quiescent, G₀-like state that is defined by acquisition of stress resistance and maintenance of viability (35). Cells were first grown in phosphate-limiting medium that contained dextrose as a carbon source (LD medium), so that there was little, if any, expression of the *top1-T722A* allele. Dense, unbudded cells were then separated from the remainder of the population using a Percoll gradient (36). Aliquots of the resulting quiescent (Q) cells were plated to measure the background frequency of Lys^+ revertants and then were maintained in a quiescent state for an additional 5 d using Q medium that contained no phosphate. The Q medium was supplemented either with galactose (QG) to induce transcription of the *pGAL-top1-T722A* allele or with dextrose (QD) to maintain its repression.

In the *pGAL-top1-T722A* strain, the frequency of Lys^+ revertants in Q cells prior to their transfer to QG medium was 1.7×10^{-7} , and there were no large deletions among 31 revertants sequenced (LD medium; Fig. 3A and *SI Appendix*, Table S4). After 5-d incubation in QG medium, the Lys^+ frequency increased to 66×10^{-7} and 80% (155/196) of reversion events were large deletions. Among the 155 deletions, 153 were confined to *LYS2*; these ranged from 7 to 613 bp, with median size of 97 bp (*SI Appendix*, Fig. S2 and Table S2). The length distribution of perfect homology at the deletion junctions of these events is shown in Fig. 3B. The most common length was 2 bp (67/155 deletions), the longest length was 8 bp (one event) and there were no events having the more extensive homology (>12 bp) expected for microhomology-mediated end-joining (37).

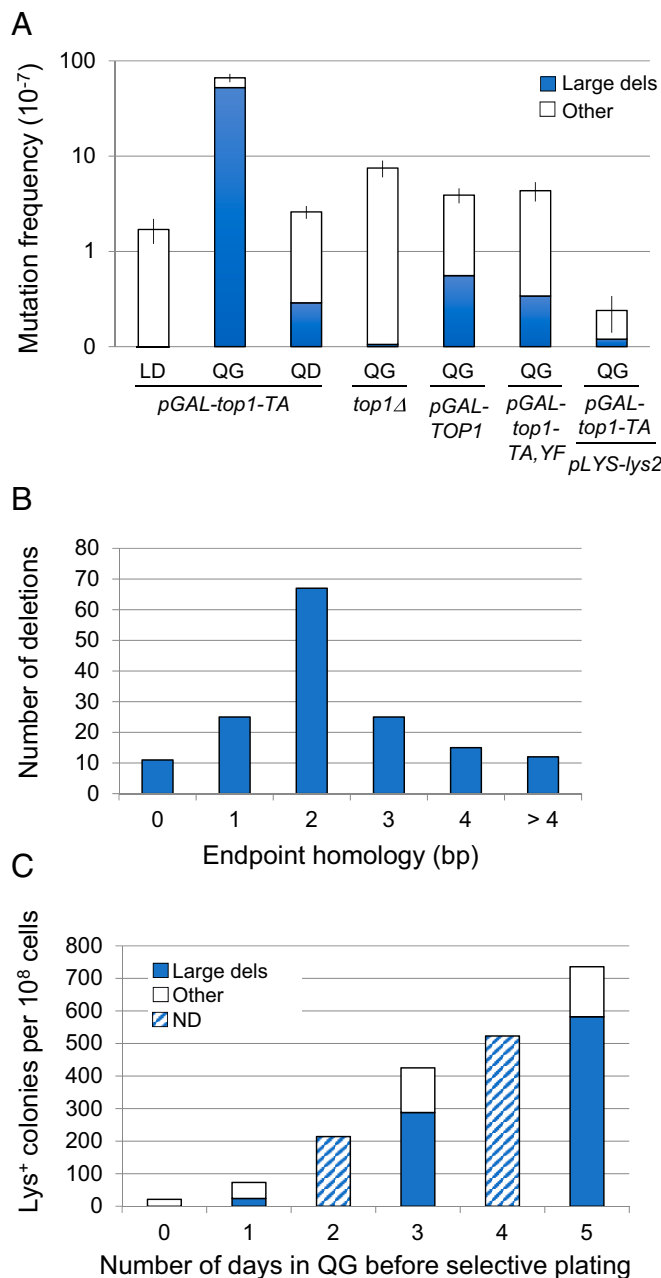


Fig. 3. Large-deletion accumulation in quiescent cells held in QG. Quiescent cells were isolated from phosphate-limiting dextrose medium (LD) and held in galactose-containing QG or dextrose-containing QD prior to selective plating on SD-lys. (A) Q cells of the indicated genotype were selectively plated after 5 d in QG or QD medium. Lys^+ frequencies and 95% confidence intervals are shown; filled blue areas represent the frequencies of large deletions. (B) The length of perfect homology at the endpoints of 155 deletions from the WT strain after 5 d in QG. (C) Time-dependent accumulation of large deletions in cells held in QG medium. Filled blue areas are the proportion of large deletions in each corresponding spectrum; cross-hatched bars indicate that a spectrum was not obtained. D0–D5 indicates days of incubation in QG medium prior to selective plating on SD-lys. Data are in *SI Appendix*, Tables S4 and S5.

The requirement of *top1-T722A* expression for large-deletion formation was confirmed by examining *pTET-lys2ΔBglNR* reversion following the incubation of *pGAL1-top1-T722A* cells in dextrose-containing QD medium, *pGAL-TOP1* cells in QG medium, or *top1Δ* cells in QG medium (Fig. 3A). We further

confirmed a requirement for Top1-T722A catalytic activity by mutating the active-site tyrosine (*pGAL1-top1-T722A,Y727F* allele) as well as the stimulatory effect of high transcription using a strain in which the *lys2ΔBglNR* allele was under the control of the endogenous *LYS2* promoter. Finally, the time dependence of *Lys*⁺ colony accumulation was examined by incubating quiescent cells for 1, 2, 3, 4, or 5 d in QG medium prior to selective plating. The accumulation of revertants was roughly linear with time (Fig. 3C and *SI Appendix, Table S5*). Although we hypothesize that the entire deletion process occurs in Q cells, microscopic examination after selective plating revealed that most cells underwent 1 to 2 divisions. It thus is possible that only the primary lesion associated with Top1-T722A expression accumulates during quiescence, with the remaining steps in deletion formation occurring after selective plating.

Genetic Control of Large Deletions in Quiescent Cells. The NHEJ dependence of large deletions that arose during growth in SG medium was recapitulated in Percoll-isolated Q cells incubated for 5 d in QG medium. In a *yku70Δ* background, the large-deletion frequency was reduced several orders of magnitude (Fig. 4) and a similar decrease was observed in a *dnl4Δ* background that lacked the dedicated NHEJ ligase, DNA ligase 4 (38). Finally, we examined the role of DNA polymerase 4 (Pol4), an X-family polymerase that is important during end/gap filling during error-prone NHEJ (39). In contrast to the complete dependence of large deletions on Ku and Dnl4, their frequency was reduced only ~3.5-fold in a *pol4Δ* background. This is consistent either with the direct joining of blunt ends, which requires no DNA synthesis, and/or the participation of alternative DNA polymerases in end/gap filling (40, 41).

Before *top1-T722A* associated ends can be joined by NHEJ, the 3'-linked Top1cc must be removed. Tdp1 is a tyrosyl-DNA phosphodiesterase that releases peptides covalently linked to 5' or 3' DNA ends, including those that remain after Top1cc proteolysis (42). In quiescent cells, *TDPI* loss was associated with only a 2.8-fold reduction in large deletions (Fig. 4), indicating involvement of additional end-processing proteins/complexes. Wss1, which is the functional homolog of the mammalian SPRTN protein (43), is a metalloprotease that degrades the protein component of DNA-protein cross-links and acts in parallel with Tdp1 to process potentially lethal Top1ccs in yeast (44). Compared to WT, there was a 2.3-fold reduction in the large-deletion frequency

in the *wss1Δ* background, which is similar to the reduction observed in the *tdp1Δ* background. In a *tdp1Δ wss1Δ* double-mutant background, however, the frequency of large deletions was reduced several orders of magnitude (Fig. 4), which is consistent with functional redundancy in Top1cc removal.

In growing cells, deletion of *EXO1* was associated with an ~4-fold increase in the large-deletion rate (Fig. 2A). By contrast, there was no change in the large-deletion frequency when *exo1Δ* Q cells were examined (Fig. 4). This is consistent with the cell cycle regulation of end resection, and its expected inefficiency outside of S phase (45). Alternatively, there may be little Exo1 that persists or is expressed in Q cells. Finally, the effect of the *mre11-D56N* nuclease-dead allele was markedly different in growing versus Q cells. Whereas there was an ~7-fold increase in the large-deletion rate in *mre11-D56N* growing cells, there was no significant change in the deletion frequency when Q cells were examined (Fig. 4). This difference likely reflects the cell cycle-dependent activation of Mre11 nuclease activity (46, 47).

Deletion of *MRE11* or *MUS81* Is Not Lethal in Q Cells Expressing Top1-T722A.

An advantage of limiting expression of Top1-T722A to quiescent cells is the potential to bypass the very slow growth and/or synthetic lethality observed in some null backgrounds. Synthetic lethality between *top1-T722A* and *MRE11* or *MUS81* deletion was previously reported (21) and was confirmed in our system. Neither an *mre11Δ* nor a *mus81Δ* strain containing the *pGAL-top1-T722A* allele was able to grow in SG medium, while both grew in SD medium. The replication-specific synthetic lethality is assumed to reflect an inability to process large numbers of replication forks that stall or collapse at Top1ccs. When Top1-T722A expression was limited to quiescent cells, the WT, *mre11Δ*, and *mus81Δ* strains had similar viability decreases (20%, 33%, and 10%, respectively) after 5 d in QG medium. In the *mre11Δ* background, the *Lys*⁺ frequency at day 5 was reduced ~25-fold, and there were no large deletions among 71 revertants sequenced. The requirement for *MRE11* is consistent with the essential role of MRX in NHEJ (48, 49). Mus81 is part of the Mus81-Mms4 structure-specific nuclease (50, 51), and in the *mus81Δ* background, there was a 4-fold reduction in the large-deletion frequency (Fig. 4).

CPT Treatment Induces Large Deletions in *pGAL-TOP1* Quiescent Cells.

To examine whether treating *TOP1* cells with CPT induced large-deletion formation, we incubated Q cells containing a *pGAL-TOP1* allele for 5 d in QG medium supplemented with 100 μM CPT dissolved in DMSO or with an equal volume of DMSO. There was no toxicity associated with CPT treatment in QG medium, consistent with the quiescent state of cells. Although the total *Lys*⁺ reversion frequency was only 2-fold higher in the presence of CPT, there was a dramatic change in the mutation spectrum upon CPT addition (*SI Appendix, Tables S2 and S4*). In the DMSO control, only a single large deletion was detected among 41 revertants analyzed. By contrast, there were 32 large deletions among 90 *Lys*⁺ colonies analyzed following incubation in the presence of CPT ($P < 0.001$).

Discussion

Stabilization of the covalent Top1cc leads to potentially toxic DSB formation during replication and in yeast, to elevated levels of homologous recombination (7, 52). An additional collateral effect is the accumulation of small 2- to 5-bp deletions that involve only nicked DNA and are DSB independent (18). In the current study, we used haploid yeast strains to more broadly examine mutagenic effects associated with stabilization of the Top1cc either by expressing the Top1-T722A protein or by adding CPT to WT cells. Regardless of the mechanism of Top1cc stabilization, NHEJ-dependent large deletions with little or no junction homology were the predominant outcome. Because of the selective system used, these deletions fell into 2 distinct classes: deletions up to ~600 bp

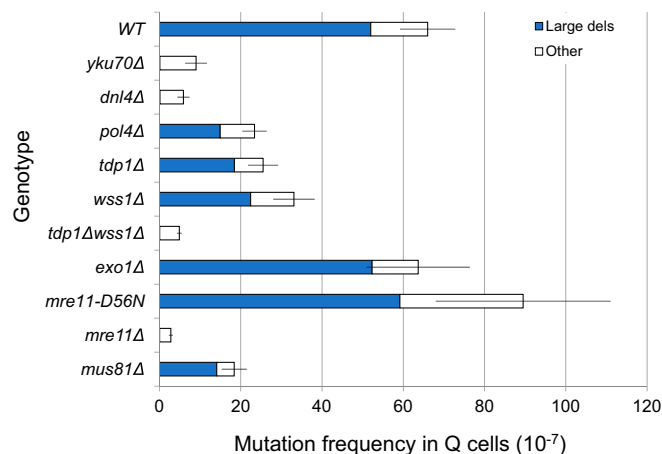


Fig. 4. Genetic requirements of Top1-T722A-associated deletions in quiescent cells. Quiescent cells were isolated from phosphate-limiting dextrose medium (LD) and held in QG medium for 5 d prior to selective plating on SD-*lys*. *Lys*⁺ frequencies and 95% confidence intervals are shown; filled blue areas are the frequencies of large deletions in each spectrum. Data are in *SI Appendix, Table S4*.

(median size, ~100 bp) that were confined to *LYS2*, and 3.2- to 4.1-kb deletions that deleted the 5' end of *LYS2* and fused the remainder of the gene to the upstream *kanMX* gene. The dispensability of the N terminus of the *Lys2* protein as well as sequence downstream of the theoretical window for compensatory changes was unexpected and further extends the flexibility of *LYS2*-based frameshift-reversion reporters. Given the requirement for the creation of a functional protein, the current analyses likely detected only a subset of deletions and their upper size limit remains unknown.

NHEJ assays in yeast typically measure the error-prone repair of a defined chromosomal DSB or the circularization of a linearized plasmid following transformation (53). In the absence of a repair template for homologous recombination, Ku-dependent NHEJ occurs efficiently. The ends are directly joined in the case of plasmid-based assays or are only slightly modified by deletion/insertion of a few base pairs to prevent reiterative cleavage in chromosomal assays. The absolute Ku dependence of the Top1-dependent deletions and the repressive effect of the *Exo1* exonuclease on these events is inconsistent with significant loss of sequence from the ends of a single DSB. We suggest instead that the events observed here reflect the NHEJ-mediated joining of ends from 2 independent DSBs. These genetic requirements, as well as the requirement for Top1 processing by *Tdp1*/*Wss1*, also exclude an alternative mechanism in which Top1 directly generates a deletion intermediate on only one DNA strand. This can occur if a given Top1cc is attacked by the 5'-OH generated by a separate aborted cleavage-ligation reaction (Fig. 5*A* and refs. 54 and 55). We note that a similar Top1-only mechanism involving sister chromatids would be expected to generate duplications as well as deletions and duplications were not detected (see below).

Our initial assumption was that the relevant DSBs were most likely generated by the encounter of 2 distinct Top1ccs with independent replication forks. There are several reasons why we disfavor this particular mechanism. First, the accumulation of

time-dependent deletions in saturated cultures, on solid medium after selective plating, and in isolated quiescent cells is suggestive of replication-independent DSB formation. Because cells undergo 1 to 2 divisions after selective plating, however, it remains possible that only the relevant Top1ccs (i.e., stabilized nicks) arise in non-dividing cells and that these are subsequently converted to DSBs upon selective plating. Second, the effects of *exo1Δ* and the *mre11-D56N* allele were different in dividing versus quiescent cells. Additionally, deletion of the *MRE11* or *MUS81* gene, which is lethal in a *top1-T722A* background, was tolerated when *top1-T722A* expression was limited to quiescent cells. Finally, as illustrated in Fig. 5*B*, if the encounter of 2 separate Top1ccs by converging replication forks breaks both sister chromatids, duplications as well as deletions are expected. Although duplications should be compatible with *Lys2* function, they strikingly were absent in the current analysis. We note, however, that if both replication-associated breaks are on the same sister chromatid (not shown), only deletions would occur. In this context, however, repair via the much more efficient recombination pathway would be expected to exclude frequent NHEJ.

If Top1-dependent DSBs are not replication-associated, then how do they arise? In vitro, DSBs can be directly generated by Top1 if one DNA strand contains a ribonucleotide (32). The first strand is broken when Top1 incises at the ribonucleotide and is released, leaving behind a nick flanked by a 2',3'-cyclic phosphate and a 5'-OH. Top1 incision of complementary strand nearby results in a DSB with the enzyme linked to the 3' end. Although the enhanced accumulation of DSBs in a genetic background that elevates ribonucleotides levels in DNA indicates that this also occurs in vivo (32), elevating the level of ribonucleotides had no effect on the large-deletion frequency in our system. As an alternative replication-independent mechanism, we suggest that the relevant DSBs can arise either when Top1 incises both DNA strands in close proximity or when Top1 nicks DNA when there is a preexisting nick on the complementary strand (Fig. 5*C*). This would be followed by Top1cc removal by *Tdp1*/*Wss1* and

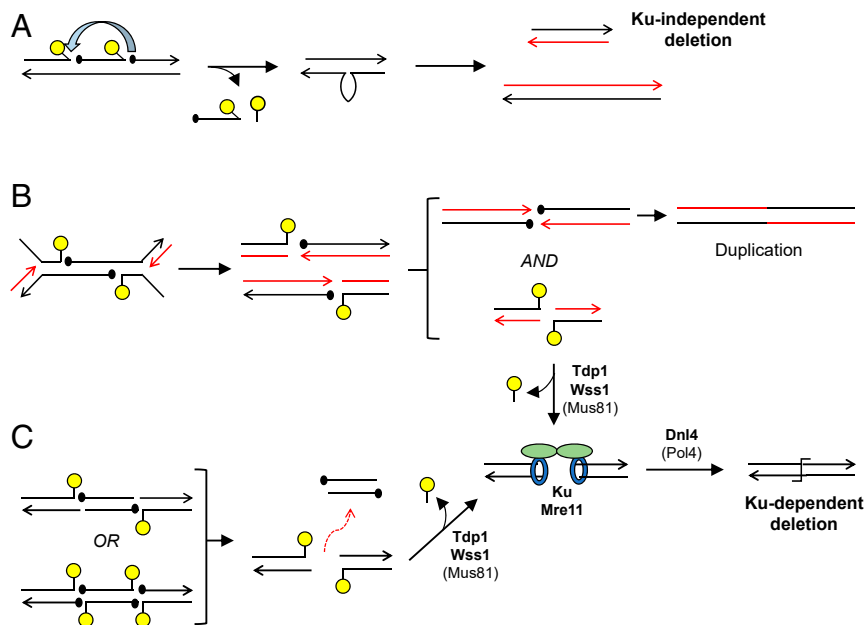


Fig. 5. Mechanisms for large-deletion formation. Deletions are initiated by 2 trapped Top1ccs (yellow lollipops); arrowheads and black circles indicate 3'-OH and 5'-OH ends, respectively. Red lines correspond to newly replicated DNA strands. (A) Top1ccs are trapped on the same DNA strand and the attack (blue arrow) of the phosphotyrosine bond of the upstream Top1cc by the 5'-OH of the second Top1cc reseals the top strand and deletes the intervening DNA segment. Because Top1 facilitates the ligation, NHEJ is not required. (B) Top1ccs are on complementary strands, and both sister chromatids are broken when encountered by converging replication forks. NHEJ-mediated ligation to the fragment from the sister chromatid generates either a deletion or duplication of the region flanked by the nicks. (C) DSBs are created when Top1 cleaves opposite random or Top1-generated nicks. The fragment between the DSBs is lost and NHEJ ligates the broken ends following Top1cc removal. Proteins involved in large-deletion formation in Q cells are indicated at the relevant step. Those that play a relatively minor role are in parentheses.

engagement of Ku for subsequent NHEJ. Although we considered the large deletions that were confined to *LYS2* and those that created a fusion protein jointly, when data from all genetic backgrounds were summed, there was significantly more of the 4-kb fusion class detected when cells were grown for 3 d in SG medium than when *top1-T722A* expression was limited to quiescent cells (21/132 and 14/543, respectively, in *SI Appendix, Table S2*; $P < 0.0001$). It is possible that this difference reflects a shift from a mostly replication-dependent mechanism to a mostly replication-independent mechanism.

NHEJ plays only a very minor role during DSB repair in yeast, and large deletions similar to those reported here were not associated with CPT treatment or *Top1-T722A* expression in a diploid strain (52). Although NHEJ is only a minor DSB repair pathway in yeast, it plays a prominent role during DSB repair in mammalian cells (56). We suggest that the *Top1cc*-dependent deletions described here are likely relevant to uncharacterized rearrangements observed 20 y ago when selecting forward mutations in mammalian cells treated with a *Top1* poison (19, 20). These may have been replication dependent in a context where NHEJ is efficient, while being largely relegated to nondividing cells in yeast. Similar *Top1*-initiated events may provide a source of genetic change in evolving cancer cells, especially following patient treatment with a *Top1* poison. In addition, a similar mechanism that is primarily transcription driven may be a potential source of genetic instability in dormant tumor cells (57) and in postmitotic tissues (58). Although the deletion size was limited to ~4 kb because of the selective system used here, larger deletions or rearrangements within/between chromosomes are expected and could be detected using an appropriate selective system.

Materials and Methods

Strain Constructions. *SI Appendix, Table S6* contains a list of the strains used in the experiments reported. All growth was at 30 °C, and 2 independent isolates of each genetic background were used to generate data. Strains were maintained as glycerol stocks at –80 °C, and all were derived from YPH45 [*MATa ura3-52 ade2-101_{oc} lys2-801_{am} trp1Δ1*], a strain congenic with S288C (59) by transformation or by mating with an isogenic strain to combine desired genetic markers. Derivatives were made by transformation or through the crossing of appropriate YPH45 derivatives of opposite mating type. The *MATα* version of YPH45 was obtained through a mating-type switch using a *pGAL-HO* plasmid. In all strains, the endogenous *LYS2* locus on chromosome II was deleted, and the full-length gene was inserted on chromosome III near *ARS306* in the orientation in which replication and transcription forks move in the same direction (60). The transplanted allele was either under control of the *LYS2* promoter or regulated by a 2-component, doxycycline-repressible *pTET-off* system (61). The *lys2ΔBglI/IR* allele (22) was derived by mutating homopolymer runs >3 N in the reversion window of the *lys2ΔBglI* allele, an allele with a 4-bp insertion generated by filling in a unique *BglII* restriction site within *LYS2* (23). The *delitto perfetto* method, which involves insertion of a selectable cassette and its subsequent replacement with a DNA fragment of interest by counterselection (62), was used to introduce the *lys2ΔBglI/IR* allele from *XhoI/AflIII*-digested pSR701 (22).

To construct the *pGAL-TOP1* allele, the promoter of *TOP1* was replaced with *pGAL1* via one-step allele replacement using a *TRP1:pGAL1* cassette amplified from plasmid pFA6a-TRP1-PGAL1 (63). *Delitto perfetto* was then used to introduce the *top1-T722A* or *top1-T722A,Y727F* allele as part of a small duplex fragment obtained by annealing complementary oligonucleotides. The *mre11-D56N* allele was introduced by 2-step allele replacement using *SphI*-digested pSM444 (64). The *TOP1*, *DNL4*, *YKU70*, *POL4*, *EXO1*, *MRE11*, *MUS81*, *TDP1*, and *WSS1* genes were deleted by 1-step allele replacement using a PCR-generated cassette amplified from a plasmid containing an appropriate selective marker. The *loxP-TRP1-loxP* disruption cassette was amplified from pSR954, which was constructed by replacing the *kanMX4* gene of pUG6 (65) with *TRP1*. The *loxP-URA3KI-loxP* cassette was amplified from pUG72 (66) and the *natMX4* marker from pAG25 (67). The *loxP-hph-loxP* cassette was amplified from pSR955, which was constructed by inserting a *BglII/SacI* fragment containing *hphMX4* (67) into *BglII/SacI*-digested pUG6 (65).

Mutation Rate and Frequency Measurements in Galactose Medium. Independent cultures were started by inoculating single colonies from YEPD

plates (1% yeast extract, 2% Bacto-peptone, 250 μg/mL adenine hemisulfate supplemented with 2% dextrose) into synthetic complete medium (6.7 g/L yeast nitrogen base plus 1.4 g of a mix of all amino acids, uracil, and adenine) supplemented with 2% galactose (SG). Following 3 d of growth, cells were washed with H₂O, and appropriate dilutions were plated onto synthetic complete dextrose medium lacking lysine (SD-lys) and YEPD to determine the total number of *Lys*⁺ revertants and the average number of cells, respectively, in each culture. Colonies were counted 3 d after plating. Mutation rates were calculated using the method of the median (68), and 95% confidence intervals were determined as described previously (69). Alternatively, the mean *Lys*⁺ frequency was calculated and the SEM was used to derive 95% confidence intervals. The rate or frequency of large deletions was estimated by multiplying the rate or frequency of *Lys*⁺ colonies by the proportion of large deletions in the corresponding spectrum.

To examine the accumulation of *Lys*⁺ revertants in saturated cultures, SG cultures were inoculated to a concentration of 20,000 cells per mL. Cells were counted daily using a hemocytometer and reached saturation 3 to 4 d after inoculation. To determine *Lys*⁺ reversion frequencies before and after cultures reached saturation, aliquots of each culture were removed 3 d and 9 or 10 d after inoculation and plated selectively and nonselectively. Following the calculation of the mutation frequency in each culture, mean frequencies, 95% confidence intervals, and large-deletion frequencies were determined as described above. Data are in *SI Appendix, Table S1*.

Time-Dependent Accumulation of Large Deletions on SD-Lys and SG-Lys Plates.

Independent cultures were grown for 4 d in SD medium to suppress *pGAL-top1-T722A* expression. Cells were washed, and appropriate dilutions were plated on YEPD plates to determine the number of viable cells in each culture. The remaining cells were plated in parallel on SD-lys and SG-lys plates, and *Lys*⁺ colony appearance was monitored over a 9-d period. On D3, D5/6, or D8/9, newly appearing *Lys*⁺ colonies were counted and DNA from representative colonies was isolated and analyzed to obtain a corresponding spectrum. Data are provided in *SI Appendix, Table S3*.

Mutation Frequencies in Quiescent Cells.

Five to 10 colonies from YPD plates were inoculated into 250 or 500 mL of phosphate-limiting L medium (0.07% phosphate-free yeast nitrogen base, 10 μg/mL KH₂PO₄, 0.1% KCl, 0.5% NH₄SO₄, 2% dextrose, 1.4 g/L complete amino acids mix) and incubated with shaking for 7 to 8 d. Cells were collected by centrifugation, washed with H₂O, resuspended in 1 mL of 50 mM Tris-HCl, pH 7.9, and sonicated for 3 min using an Isonic Digital Ultrasonic Cleaner. Percoll gradients were made by mixing 1 part 1.5 M NaCl with 9 parts Percoll (density 1.130 g/mL; GE Healthcare), and 25 mL were distributed into 30-mL glass conical tubes. Tubes were centrifuged for 15 min at 13,800 rpm at 20 °C in a fixed-angle Sorvall SS-34 rotor. Cells were loaded onto Percoll gradients and centrifuged for 1 h at 400 rcf in a swinging bucket rotor (Eppendorf centrifuge 5810R) at 20 °C. After centrifugation, quiescent cells were taken from the bottom fraction, washed with H₂O, and counted in a hemocytometer. Appropriate dilutions were plated on YEPD to determine viability and on SD-lys to determine the number of preexisting revertants following incubation in L medium. Cells were then pelleted and resuspended in phosphate-free Q medium (0.07% phosphate-free yeast nitrogen base, 0.1% KCl, 0.5% NH₄SO₄, 1.4 g/L complete amino acids mix) containing either 2% dextrose or 2% galactose (QD and QG, respectively). Following incubation of QG or QD cultures on a roller drum for the appropriate time period, cells were washed and appropriate dilutions were plated on YEPD and SD-lys in order to determine total viable cells and *Lys*⁺ revertants, respectively, in each culture. Colonies were counted 3 d postplating, and mean *Lys*⁺ frequencies, 95% confidence intervals, and large-deletion frequencies were determined as described above. Data from Q-medium experiments are in *SI Appendix, Tables S4 and S5*.

Mutation Spectra. For SG liquid cultures, only a single colony was selected from each culture to ensure independence. For SG-lys plate experiments and Q-media experiments in which cells were not dividing, multiple *Lys*⁺ colonies were analyzed from a single plate/culture. Following genomic DNA isolation, the *lys2* reversion window was amplified using forward primer *LYSWINF* (5'-GCCTCATGATAGTTTTCTAACAAATACG) or *Lys2ATG* (5'-GACTAACGAAAA-GGTCTGGATAG) with reverse primer *LYSWINR* (5'-CCCATCACACATACCA-TCAAATCCAC). If the initial PCR failed, a product was obtained using primer *Lys2F14* (5'-CACAGTTTTAGCGAGG) and *LYSWINR*. PCR products were sequenced using the forward or reverse primer used for amplification. Sequencing was done by the Duke University DNA Analysis Facility, Eurofins MWG Operon, or Eton Bioscience. Sequences were analyzed using DNASTAR Seqman Pro, SnapGene Viewer, BEdit, and Python. Deletions confined to *LYS2* ORF were aligned using DNASTAR Seqman Pro and pasted into BEdit to save as a raw txt file for Python analysis. A Python script (70) was written to export CVS files containing deletion start sites, sizes, junction identities, and the number of occurrences of

each deletion. Python also was used to generate JPG files of individual deletion spectra. The 3.2- to 4.1-kb deletions were analyzed using Seqman Pro and SnapGene Viewer; deletion endpoints, sizes, and junction identities were manually determined and plotted using Python. Coordinates of the deletions detected in different genetic backgrounds and/or media types are given in *SI Appendix, Table S2*. Corresponding graphical summaries of 3.2- to 4.1-kb deletions and deletions confined to the *lys2ΔBtgNR* reversion window are presented in *SI Appendix, Figs. S1 and S2*, respectively.

Data Availability. All data discussed in the paper are in the *SI Appendix*.

ACKNOWLEDGMENTS. We thank Alex Neil and Sergei Mirkin for sharing their procedure for isolating quiescent cells following phosphate starvation; Karen O'Connell and Muthana Al Abo for their help in writing Python scripts; and Tom Petes for comments on the manuscript. This work was supported by a grant to S.J.-R. from the National Institutes of Health (R35 GM203587).

1. Y. Pommier, Y. Sun, S. N. Huang, J. L. Nitiss, Roles of eukaryotic topoisomerases in transcription, replication and genomic stability. *Nat. Rev. Mol. Cell Biol.* **17**, 703–721 (2016).
2. Y. Fan, J. N. Weinstein, K. W. Kohn, L. M. Shi, Y. Pommier, Molecular modeling studies of the DNA-topoisomerase I ternary cleavable complex with camptothecin. *J. Med. Chem.* **41**, 2216–2226 (1998).
3. Y. H. Hsiang, R. Hertzberg, S. Hecht, L. F. Liu, Camptothecin induces protein-linked DNA breaks via mammalian DNA topoisomerase I. *J. Biol. Chem.* **260**, 14873–14878 (1985).
4. M. R. Redinbo, L. Stewart, P. Kuhn, J. J. Champoux, W. G. Hol, Crystal structures of human topoisomerase I in covalent and noncovalent complexes with DNA. *Science* **279**, 1504–1513 (1998).
5. Y. Pommier, Drugging topoisomerases: Lessons and challenges. *ACS Chem. Biol.* **8**, 82–95 (2013).
6. W. K. Eng, L. Faucette, R. K. Johnson, R. Sternglanz, Evidence that DNA topoisomerase I is necessary for the cytotoxic effects of camptothecin. *Mol. Pharmacol.* **34**, 755–760 (1988).
7. J. Nitiss, J. C. Wang, DNA topoisomerase-targeting antitumor drugs can be studied in yeast. *Proc. Natl. Acad. Sci. U.S.A.* **85**, 7501–7505 (1988).
8. S. J. Boulton, S. P. Jackson, *Saccharomyces cerevisiae* Ku70 potentiates illegitimate DNA double-strand break repair and serves as a barrier to error-prone DNA repair pathways. *EMBO J.* **15**, 5093–5103 (1996).
9. M. J. Lippert *et al.*, Role for topoisomerase 1 in transcription-associated mutagenesis in yeast. *Proc. Natl. Acad. Sci. U.S.A.* **108**, 698–703 (2011).
10. T. Takahashi, G. Burguiere-Slezak, P. A. Van der Kemp, S. Boiteux, Topoisomerase I provokes the formation of short deletions in repeated sequences upon high transcription in *Saccharomyces cerevisiae*. *Proc. Natl. Acad. Sci. U.S.A.* **108**, 692–697 (2011).
11. J. E. Cho, N. Kim, Y. C. Li, S. Jinks-Robertson, Two distinct mechanisms of topoisomerase 1-dependent mutagenesis in yeast. *DNA Repair (Amst.)* **12**, 205–211 (2013).
12. N. Kim *et al.*, Mutagenic processing of ribonucleotides in DNA by yeast topoisomerase I. *Science* **332**, 1561–1564 (2011).
13. J. E. Cho *et al.*, Parallel analysis of ribonucleotide-dependent deletions produced by yeast Top1 *in vitro* and *in vivo*. *Nucleic Acids Res.* **44**, 7714–7721 (2016).
14. S. Y. Huang, S. Ghosh, Y. Pommier, Topoisomerase I alone is sufficient to produce short DNA deletions and can also reverse nicks at ribonucleotide sites. *J. Biol. Chem.* **290**, 14068–14076 (2015).
15. J. L. Sparks, P. M. Burgers, Error-free and mutagenic processing of topoisomerase 1-provoked damage at genomic ribonucleotides. *EMBO J.* **34**, 1259–1269 (2015).
16. W. C. Colley, M. van der Merwe, J. R. Vance, A. B. Burgin, Jr, M. A. Bjornsti, Substitution of conserved residues within the active site alters the cleavage religation equilibrium of DNA topoisomerase I. *J. Biol. Chem.* **279**, 54069–54078 (2004).
17. M. D. Magonigal, J. Fertala, M. A. Bjornsti, Alterations in the catalytic activity of yeast DNA topoisomerase I result in cell cycle arrest and cell death. *J. Biol. Chem.* **272**, 12801–12808 (1997).
18. R. Sloan, S. N. Huang, Y. Pommier, S. Jinks-Robertson, Effects of camptothecin or TOP1 overexpression on genetic stability in *Saccharomyces cerevisiae*. *DNA Repair (Amst.)* **59**, 69–75 (2017).
19. E. Balestrieri, R. Zanier, F. Degrassi, Molecular characterisation of camptothecin-induced mutations at the *hprt* locus in Chinese hamster cells. *Mutat. Res.* **476**, 63–69 (2001).
20. H. Hashimoto, S. Chatterjee, N. A. Berger, Mutagenic activity of topoisomerase I inhibitors. *Clin. Cancer Res.* **1**, 369–376 (1995).
21. R. J. Reid *et al.*, Selective ploidy ablation, a high-throughput plasmid transfer protocol, identifies new genes affecting topoisomerase I-induced DNA damage. *Genome Res.* **21**, 477–486 (2011).
22. K. Lehner, S. V. Mudrak, B. K. Minesinger, S. Jinks-Robertson, Frameshift mutagenesis: The roles of primer-template misalignment and the nonhomologous end-joining pathway in *Saccharomyces cerevisiae*. *Genetics* **190**, 501–510 (2012).
23. C. N. Greene, S. Jinks-Robertson, Frameshift intermediates in homopolymer runs are removed efficiently by yeast mismatch repair proteins. *Mol. Cell Biol.* **17**, 2844–2850 (1997).
24. H. P. Phatnani, J. C. Jones, A. L. Greenleaf, Expanding the functional repertoire of CTD kinase I and RNA polymerase II: Novel phosphoCTD-associating proteins in the yeast proteome. *Biochemistry* **43**, 15702–15719 (2004).
25. J. Wu, H. P. Phatnani, T. S. Hsieh, A. L. Greenleaf, The phosphoCTD-interacting domain of topoisomerase I. *Biochem. Biophys. Res. Commun.* **397**, 117–119 (2010).
26. T. T. Paull, 20 years of Mre11 biology: No end in sight. *Mol. Cell* **71**, 419–427 (2018).
27. S. Moreau, J. R. Ferguson, L. S. Symington, The nuclease activity of Mre11 is required for meiosis but not for mating type switching, end joining, or telomere maintenance. *Mol. Cell Biol.* **19**, 556–566 (1999).
28. E. P. Mimitou, L. S. Symington, Ku prevents Exo1 and Sgs1-dependent resection of DNA ends in the absence of a functional MRX complex or Sae2. *EMBO J.* **29**, 3358–3369 (2010).
29. N. K. Hamilton, N. Maizels, MRE11 function in response to topoisomerase poisons is independent of its function in double-strand break repair in *Saccharomyces cerevisiae*. *PLoS One* **5**, e15387 (2010).
30. L. R. Myler *et al.*, Single-molecule imaging reveals how Mre11-Rad50-Nbs1 initiates DNA break repair. *Mol. Cell* **67**, 891–898.e4 (2017).
31. S. S. Foster, A. Balestrini, J. H. Petrini, Functional interplay of the Mre11 nuclease and Ku in the response to replication-associated DNA damage. *Mol. Cell Biol.* **31**, 4379–4389 (2011).
32. S. N. Huang, J. S. Williams, M. E. Arana, T. A. Kunkel, Y. Pommier, Topoisomerase I-mediated cleavage at unrepaired ribonucleotides generates DNA double-strand breaks. *EMBO J.* **36**, 361–373 (2017).
33. S. A. Nick McElhinny *et al.*, Genome instability due to ribonucleotide incorporation into DNA. *Nat. Chem. Biol.* **6**, 774–781 (2010).
34. M. M. Klosinska, C. A. Crutchfield, P. H. Bradley, J. D. Rabinowitz, J. R. Broach, Yeast cells can access distinct quiescent states. *Genes Dev.* **25**, 336–349 (2011).
35. J. V. Gray *et al.*, “Sleeping beauty”: Quiescence in *Saccharomyces cerevisiae*. *Microbiol. Mol. Biol. Rev.* **68**, 187–206 (2004).
36. C. Allen *et al.*, Isolation of quiescent and nonquiescent cells from yeast stationary-phase cultures. *J. Cell Biol.* **174**, 89–100 (2006).
37. D. D. Villarreal *et al.*, Microhomology directs diverse DNA break repair pathways and chromosomal translocations. *PLoS Genet.* **8**, e1003026 (2012).
38. S. H. Teo, S. P. Jackson, Identification of *Saccharomyces cerevisiae* DNA ligase IV: Involvement in DNA double-strand break repair. *EMBO J.* **16**, 4788–4795 (1997).
39. J. M. Daley, R. L. Laan, A. Suresh, T. E. Wilson, DNA joint dependence of pol X family polymerase action in nonhomologous end joining. *J. Biol. Chem.* **280**, 29030–29037 (2005).
40. C. Y. Chan, A. Galli, R. H. Schiestl, Pol3 is involved in nonhomologous end-joining in *Saccharomyces cerevisiae*. *DNA Repair (Amst.)* **7**, 1531–1541 (2008).
41. S. F. Tseng, A. Gabriel, S. C. Teng, Proofreading activity of DNA polymerase Pol2 mediates 3'-end processing during nonhomologous end joining in yeast. *PLoS Genet.* **4**, e1000060 (2008).
42. J. J. Pouliot, K. C. Yao, C. A. Robertson, H. A. Nash, Yeast gene for a Tyr-DNA phosphodiesterase that repairs topoisomeric I complexes. *Science* **286**, 552–555 (1999).
43. J. Fielden, A. Ruggiano, M. Popovic, K. Ramadan, DNA protein crosslink proteolysis repair: From yeast to premature ageing and cancer in humans. *DNA Repair (Amst.)* **71**, 198–204 (2018).
44. J. Stinglele, M. S. Schwarz, N. Bloemeke, P. G. Wolf, S. Jentsch, A DNA-dependent protease involved in DNA-protein crosslink repair. *Cell* **158**, 327–338 (2014).
45. L. S. Symington, End resection at double-strand breaks: Mechanism and regulation. *Cold Spring Harb. Perspect. Biol.* **6**, a016436 (2014).
46. P. Huertas, F. Cortés-Ledesma, A. A. Sartori, A. Aguilera, S. P. Jackson, CDK targets Sae2 to control DNA-end resection and homologous recombination. *Nature* **455**, 689–692 (2008).
47. E. Cannavo *et al.*, Regulatory control of DNA end resection by Sae2 phosphorylation. *Nat. Commun.* **9**, 4016 (2018).
48. S. J. Boulton, S. P. Jackson, Components of the Ku-dependent non-homologous end-joining pathway are involved in telomeric length maintenance and telomeric silencing. *EMBO J.* **17**, 1819–1828 (1998).
49. J. K. Moore, J. E. Haber, Cell cycle and genetic requirements of two pathways of nonhomologous end-joining repair of double-strand breaks in *Saccharomyces cerevisiae*. *Mol. Cell Biol.* **16**, 2164–2173 (1996).
50. S. A. Bastin-Shanower, W. M. Fricke, J. R. Mullen, S. J. Brill, The mechanism of Mus81-Mms4 cleavage site selection distinguishes it from the homologous endonuclease Rad1-Rad10. *Mol. Cell Biol.* **23**, 3487–3496 (2003).
51. K. T. Ehmsen, W. D. Heyer, *Saccharomyces cerevisiae* Mus81-Mms4 is a catalytic, DNA structure-selective endonuclease. *Nucleic Acids Res.* **36**, 2182–2195 (2008).
52. S. L. Andersen, R. S. Sloan, T. D. Petes, S. Jinks-Robertson, Genome-destabilizing effects associated with top1 loss or accumulation of top1 cleavage complexes in yeast. *PLoS Genet.* **11**, e1005098 (2015).
53. J. M. Daley, P. L. Palmbo, D. Wu, T. E. Wilson, Nonhomologous end joining in yeast. *Annu. Rev. Genet.* **39**, 431–451 (2005).
54. K. A. Henningfeld, S. M. Hecht, A model for topoisomerase I-mediated insertions and deletions with duplex DNA substrates containing branches, nicks, and gaps. *Biochemistry* **34**, 6120–6129 (1995).
55. N. Kim, S. Jinks-Robertson, The Top1 paradox: Friend and foe of the eukaryotic genome. *DNA Repair (Amst.)* **56**, 33–41 (2017).
56. E. M. Kass, M. Jasin, Collaboration and competition between DNA double-strand break repair pathways. *FEBS Lett.* **584**, 3703–3708 (2010).
57. S. Kleffel, T. Schatton, Tumor dormancy and cancer stem cells: Two sides of the same coin? *Adv. Exp. Med. Biol.* **734**, 145–179 (2013).
58. P. J. McKinnon, Topoisomerases and the regulation of neural function. *Nat. Rev. Neurosci.* **17**, 673–679 (2016).
59. R. S. Sikorski, P. Hieter, A system of shuttle vectors and yeast host strains designed for efficient manipulation of DNA in *Saccharomyces cerevisiae*. *Genetics* **122**, 19–27 (1989).

60. N. Kim, A. L. Abdulovic, R. Gealy, M. J. Lippert, S. Jinks-Robertson, Transcription-associated mutagenesis in yeast is directly proportional to the level of gene expression and influenced by the direction of DNA replication. *DNA Repair (Amst.)* **6**, 1285–1296 (2007).
61. G. Belli, E. Gari, M. Aldea, E. Herrero, Functional analysis of yeast essential genes using a promoter-substitution cassette and the tetracycline-regulatable dual expression system. *Yeast* **14**, 1127–1138 (1998).
62. F. Storic, M. A. Resnick, The *delitto perfetto* approach to *in vivo* site-directed mutagenesis and chromosome rearrangements with synthetic oligonucleotides in yeast. *Methods Enzymol.* **409**, 329–345 (2006).
63. M. S. Longtine *et al.*, Additional modules for versatile and economical PCR-based gene deletion and modification in *Saccharomyces cerevisiae*. *Yeast* **14**, 953–961 (1998).
64. B. Llorente, L. S. Symington, The Mre11 nuclease is not required for 5' to 3' resection at multiple HO-induced double-strand breaks. *Mol. Cell. Biol.* **24**, 9682–9694 (2004).
65. U. Guldener, S. Heck, T. Fielder, J. Beinhauer, J. H. Hegemann, A new efficient gene disruption cassette for repeated use in budding yeast. *Nucleic Acids Res.* **24**, 2519–2524 (1996).
66. U. Guldener, J. Heinisch, G. J. Koehler, D. Voss, J. H. Hegemann, A second set of *loxP* marker cassettes for Cre-mediated multiple gene knockouts in budding yeast. *Nucleic Acids Res.* **30**, e23 (2002).
67. A. L. Goldstein, J. H. McCusker, Three new dominant drug resistance cassettes for gene disruption in *Saccharomyces cerevisiae*. *Yeast* **15**, 1541–1553 (1999).
68. D. E. Lea, C. A. Coulson, The distribution of the numbers of mutants in bacterial populations. *J. Genet.* **49**, 264–285 (1949).
69. R. M. Spell, S. Jinks-Robertson, Determination of mitotic recombination rates by fluctuation analysis in *Saccharomyces cerevisiae*. *Methods Mol. Biol.* **262**, 3–12 (2004).
70. J.-E. Cho, M. Al Abo, MHfinderatDelJct. Github. <https://github.com/muthalpy/MHfinderatDelJct>. git. Deposited 10 October 2019.